DOI: 10.1002/anie.201002418

Water Wires

Water Chains in Hydrophobic Crystal Channels: Nanoporous Materials as Supramolecular Analogues of Carbon Nanotubes**

*Ramalingam Natarajan, Jonathan P. H. Charmant, A. Guy Orpen, and Anthony P. Davis**

The behavior of water in narrow apolar pores has attracted much recent interest. Although it might seem that such channels should repel water,[1] it transpires that they can be hydrated and moreover that their "hydrophobic" nature promotes rapid water flow. The phenomenon is observed in biology, where the pores of aquaporins (water-transporting proteins) are composed largely of hydrophobic amino acids.[2] It is also seen for carbon nanotubes (CNTs) which, according to both theoretical[3] and experimental[4] studies, allow rapid passage of water molecules. Water flow through CNTs can be selective[5] and controllable,[6] suggesting applications in water-purification[7] and nanofluidic devices.

To understand these systems, it is important to gather structural information on water in hydrophobic environments. Especially relevant is the "water wire", a one-dimensional hydrogen-bonded chain of water molecules. The water in aquaporin channels adopts this motif,[2] as does the water in the narrowest and best-understood CNTs.[3a,b,e] However, while there are many crystal structures which show water molecules in single file,[8] there is limited information on water wires in purely hydrophobic environments.[9] In particular there seem to be no structures in which water wires are surrounded exclusively by π systems. We now report the crystal engineering of channels bounded by nonpolar aromatic units, and the structural characterization of linear chains of water molecules within these pores.

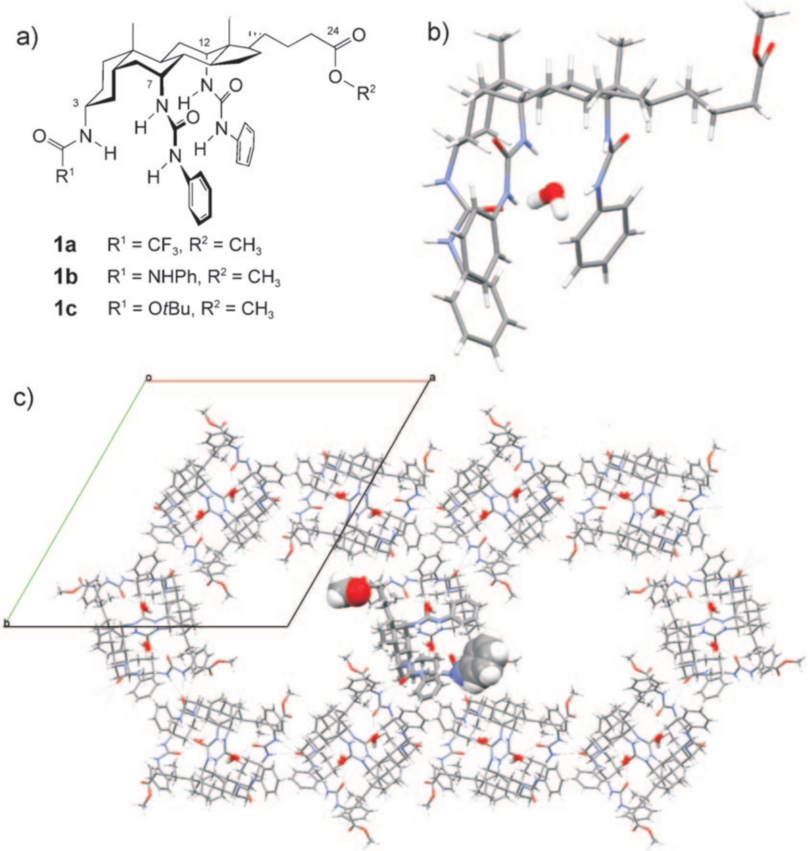

Figure 1. a) Previously described steroidal bis-phenylureas forming nanoporous crystals. b) The structure of **1b** in the crystal, showing the bound water molecule. c) Packing diagram for **1b** viewed along the axis of the channels. A single steroid is highlighted in the centre of the diagram, showing how the ester CH_3 groups form part of the surface of one channel while the C3-terminal NHPh groups protrude into another. The ester CH_3 and C3 NHPh groups are shown in space-filling mode. Also highlighted are the water molecules bound to each unit of **1b**.

We have previously shown that steroidal bis-phenylureas **1** (Figure 1a) crystallize as monohydrates to form structures with hexagonal $P6_1$ symmetry, containing one-dimensional channels of unusually large diameter (Figure 1b,c).[10] Groups R^1 and R^2 are directed into the channels, so that in principle they can be varied substantially without disrupting the crystal packing. Potentially, this should allow a broad scope for tuning of channel size and properties. Indeed, our original report[10] described three structures **1a–c**, in which group R^1 was altered to give pore diameters of 14.3, 12.3, and 11.6 Å, respectively.

Having shown that R^1 could be varied, we sought to confirm that ester group CO_2R^2 could also be used to tune the properties of the crystals. Included among our targets were steroids **2–4**, featuring large aromatic groups linked to C24–O via two-carbon tethers. Modeling suggested that this arrangement would allow the aromatic groups to lie roughly parallel to the channel axis, lining the walls and reducing the diameters to about 6 to 7 Å. We could thus create an environment not dissimilar to that inside a CNT.[11] Esters **2–4**

---

[*] Dr. R. Natarajan, Dr. J. P. H. Charmant, Prof. A. G. Orpen, Prof. A. P. Davis
School of Chemistry, University of Bristol
Cantock's Close, Bristol, BS8 1TS (UK)
Fax: (+44) 117-929-8611
E-mail: anthony.davis@bristol.ac.uk

[**] This work was supported by the EPSRC (EP/E021581/1). We thank Drs. G. Whittell and M. F. Haddow for assistance with TGA and X-ray crystallography, respectively.

Supporting information for this article is available on the WWW under http://dx.doi.org/10.1002/anie.201002418.

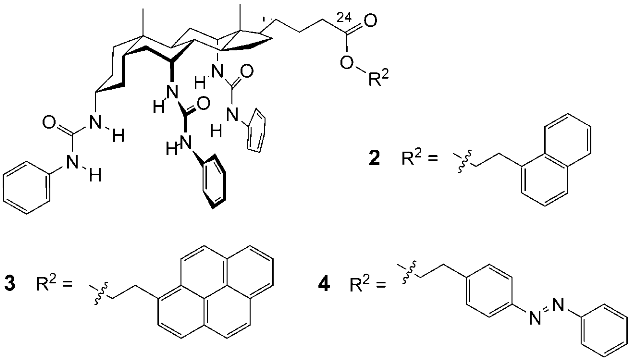

were synthesized from **1b** by methyl ester hydrolysis followed by O alkylation of the resulting carboxylate.[12] In each case needlelike crystals were obtained through slow evaporation from acetone–water or methyl acetate–water mixtures, and were subjected to X-ray crystallography at 100 K.

The crystal structures obtained for **2**–**4** were isostructural with those of **1**. As expected, the ester aromatic units came together in the channel region of the structures, essentially defining the walls of the pores (see Figure 2). Adjacent aromatic groups overlapped in a helical sequence, like scales applied to a tightly curved surface. Despite the hydrophobicity of the channels, no organic solvent was included. Instead, the crystallography detected electron density in the channels consistent with one water molecule per steroid. The presence of water in the channels was confirmed by thermogravimetric analysis (TGA) of the freshly grown air-dried crystals. In each case the TGA trace revealed weight loss equivalent to two molecules of water per steroid, occurring mainly between 140 and 170 °C with stabilization at about 180 °C.[12] Loss of two water molecules per steroid is expected, one from the pore and the other from the individual steroidal binding sites (see Figure 1).

Considered in detail, the crystal structure of **2**[13] features naphthyl units making edge-to-face contact with an interplane angle of 59° (Figure 2a). The structure appears to gain stabilization from C–H···π interactions ($d_{\text{C–H}\cdots\pi(\text{centroid})} = 2.8$ and 2.9 Å and $\theta_{\text{C–H}\cdots\pi(\text{centroid})} = 133$ and 143°). The pore diameter ranges from 5.5 to 6.6 Å. The naphthyl groups (the smallest studied in this work) are not quite large enough to provide a continuous coating for the pore, so that gaps of about 2.4 Å appear between turns of the helices (Figure 2d). However these gaps do not reveal any polar groups, so that

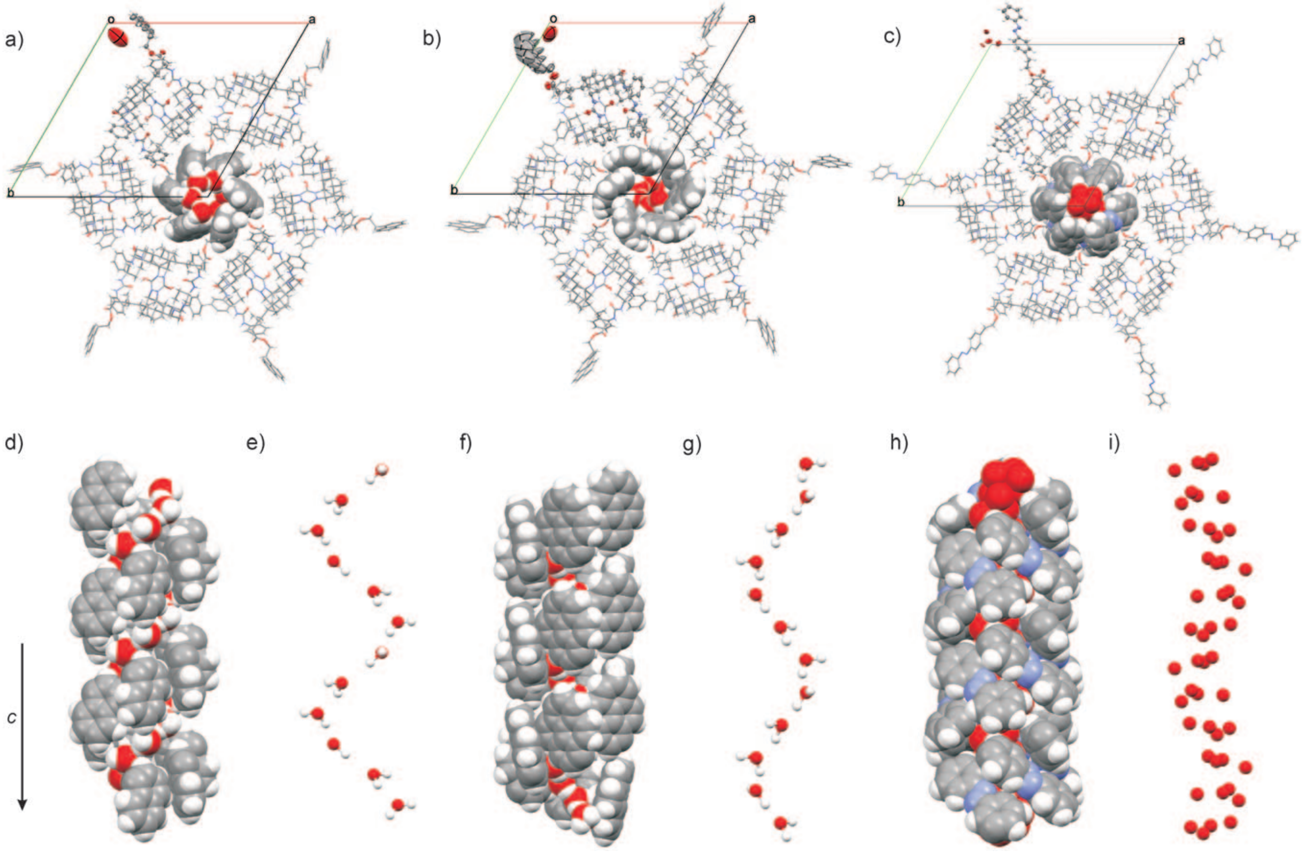

Figure 2. a–c) Crystal structures of **2**, **3**, and **4**, respectively, viewed along the *c* axis. Thermal ellipsoids (50% probability level) are shown for one asymmetric unit in each case, at the top left of each diagram. The aryl groups which line the channels, and the enclosed water molecules, are shown in space-filling mode. Water-wire hydrogen atoms in **2** and **3** were inserted and positioned by modeling, as discussed in the text. In the case of **4**, all four water positions are shown as occupied. d,f,h) Crystal structures of **2**, **3**, and **4**, respectively, viewed perpendicular to the *c* axis. Three unit cells are represented in each case. Only channel-enclosed water and surrounding aryl groups are shown. e,g,i) Channel-enclosed water positions for **2**, **3**, and **4**, respectively, viewed perpendicular to the *c* axis. Two unit cells are represented in each case.

the channel is entirely hydrophobic. The naphthyl units show modest disorder or thermal motion (mean square atomic displacement $U_{eq} = 0.09–0.15\ Å^2$; see Figure S1 in the Supporting Information), which is not unexpected considering their position at the channel surface. The water molecules within the pore form helical chains which follow the lines of the interstices between the naphthyl helices. Displacement parameters are large (U_{eq} of water oxygen atoms $= 0.79\ Å^2$), so the water molecules cannot be located precisely. However, the distance between the centroids (3.15 Å) is well within the normal range for O–H···O hydrogen bonding.[9a] The water chain (Figure 2e) was modeled with the assistance of Materials Studio software.[14] Water hydrogen atoms were added to the oxygen atoms and then allowed to move[15] in an energy minimization with periodic boundary conditions employing the COMPASS 27 force field with Ewald option. The minimization yielded a water wire with O–H···O angles of 160° and hydrogen bonding distances (H···O) of 2.22 Å. The extra-chain hydrogen atoms were positioned in the groove separating the turns of the naphthyl helix, roughly equidistant (ca. 3 Å) from three naphthyl hydrogen atoms (Figure 3a).

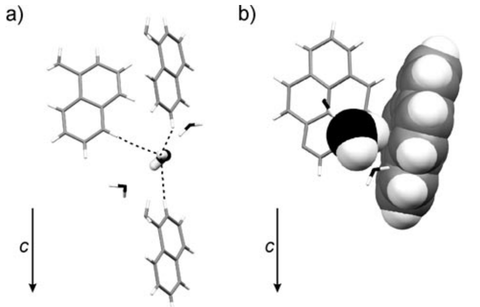

Figure 3. Environments of water-wire molecules in **2** (a) and **3** (b) from crystallography and modeling. In (a), dotted lines represent close contacts between OH and naphthyl hydrogen atoms (2.9–3.1 Å). In (b), the proposed O–H···π contact between pyrene and water wire is visualized in space-filling mode.

The crystal structure of pyrenylethyl ester **3**[16] (Figure 2b) reveals a similar assembly of aromatic units, with an angle of 58.54° between the pyrene planes. Again, the structure appears to be stabilized by C–H···π interactions between neighboring aryl units. Unlike the naphthyl groups in **2** the larger pyrene unit is capable of lining the pore surface without leaving substantial gaps (Figure 2f). The pore diameter ranges from 6.4 to 7.6 Å. Despite the apparently favorable packing, the pyrene carbon atoms show large displacement parameters ($U_{eq} = 0.43–0.67\ Å^2$), indicating significant disorder or thermal motion (Figure S2 in the Supporting Information). The water molecules occupying the pores form helical chains (Figure 2g) and also show large displacement parameters (U_{eq} of water oxygen atoms $= 0.66\ Å^2$). In contrast to **2**, the water wire passes close to the centroids of the aromatic surfaces. The distance between the water oxygen atoms is also shorter (2.6 Å). Although this is low for hydrogen-bonded water molecules, the same spacing has been proposed for a water wire in an aliphatic crystal environment.[9a] Modeling of the water hydrogen atom positions, as for **2**, yielded a structure with O–H···O angles of 156° and hydrogen bonding H···O distances of 1.64 Å. As shown in Figure 3b, the water wire takes part in O–H···π interactions with the pyrene π surfaces.[17] However this model is tentative, given the uncertainties surrounding both water and pyrene positions. Structures in which the water wire and pyrene units lack 6-fold screw symmetry are also possible, as highlighted by the case of **4** discussed below.

In the crystal structure of **4**,[18] the *trans*-diazobenzene fragments overlap in a continuous fashion, defining a channel of diameter 5.7 Å (minimum) to 8.7 Å (maximum) (Figure 2c,h). The channel-enclosed water molecules were found in four positions in the asymmetric unit, each with 25% occupancy (Figure 2i, Figure 4a). As shown in Figure 4a, three of the positions form a roughly equilateral triangle in a plane nearly perpendicular to the channel axis, while the fourth lies at the approximate centre of this triangle. The water positions were quite precisely defined, with an average U_{eq} of $0.094\ Å^2$. Random occupation of these sites is unrealistic, as many of the O···O distances between successive asymmetric units would be too small (Table S1 in the Supporting Information). Certain sequences must therefore be preferred and, given the equal occupancy of all four positions, a regular structure with an $(H_2O)_4$ repeat unit seems probable. Of the six possible sequences, five require at least one O···O distance of 2.2 Å or less.[12] The remaining option (CBDA, Figure 4b) was therefore considered the most likely. To model the water wire, twelve oxygen atoms were positioned according to this sequence, encompassing three cycles of the water chain and two unit cells of the crystal. Hydrogen atoms were added and their positions were energy-minimized using periodic boundary conditions.[15] The resulting structure is shown in Figure 4c,d. The extra-chain hydrogen atoms are placed in a variety of situations, being directed towards the benzenoid aromatic surfaces, the N=N π surface, or the CH groups. All the environments are essentially apolar; although there is potential for H-bonding to azo nitrogen lone pairs, none of the OH groups is properly positioned for such an interaction.

In conclusion, we have shown that crystal engineering with nanoporous steroids **1** can be extended to create pores with aromatic internal surfaces. To an approximation, these materials can be seen as supramolecular analogues of carbon nanotubes, employing overlapping planar aromatic surfaces to mimic the continuous curved π system inside a CNT. Although the mimicry is by no means perfect, crystallinity confers a key advantage in that detailed structures can be obtained. The observation of water wires within the pores illustrates the value of this approach. The properties of water in CNTs have attracted much attention, driven by theoretical interest and potential applications, but relevant structural data have been scarce. This work has provided the first characterization of water wires in environments similar to CNT interiors (that is, surrounded by apolar aromatic units). More generally it contributes to the understanding of water in nonpolar environments, including the water chains found in aquaporins. In future work we hope to show that nanoporous

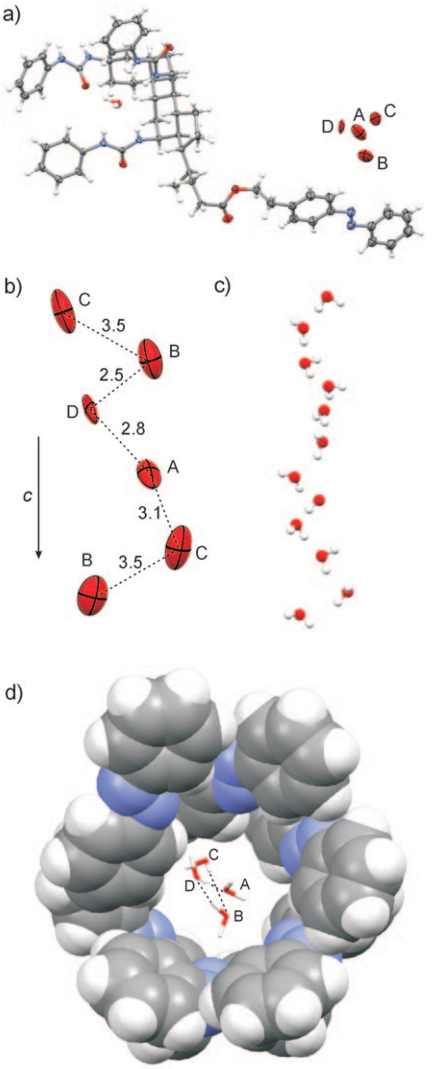

Figure 4. Modeling of the water wire in **4**. a) The asymmetric unit from crystallography, viewed down the *c* axis, showing the four environments for water molecules within the pore (labelled A–D, each with 25 % occupation). Non-hydrogen atoms are shown as thermal ellipsoids. b) The sequence of water environments proposed for the water wire, viewed perpendicular to the *c* axis. O···O distances are shown in Å. Water oxygen atoms are shown as thermal ellipsoids. c) Modeled water wire, based on the CBDA sequence. The twelve water molecules shown inhabit two unit cells of the crystal. d) One repeat unit of the water wire with neighboring azobenzene groups, viewed along a line close to the *c* axis, with the sequence CBDA heading out of the page. Hydrogen bonds are shown as dotted lines.

steroidal crystals can be engineered for a range of other characteristics, including corrugated surfaces and polar/charged interiors.

Received: April 23, 2010

Keywords: crystal engineering · hydrogen bonding · hydrophobic effect · supramolecular chemistry · water chains

---

[1] M. S. P. Sansom, P. C. Biggin, *Nature* **2001**, *414*, 156; S. Granick, S. C. Bae, *Science* **2008**, *322*, 1477.

[2] P. Agre, *Angew. Chem.* **2004**, *116*, 4377; *Angew. Chem. Int. Ed.* **2004**, *43*, 4278; D. D. Kozono, M. Yasui, L. S. King, P. Agre, *J. Clin. Invest.* **2002**, *109*, 1395; for a functional aquaporin model see: M. S. Kaucher, M. Peterca, A. E. Dulcey, A. J. Kim, S. A. Vinogradov, D. A. Hammer, P. A. Heiney, V. Percec, *J. Am. Chem. Soc.* **2007**, *129*, 11698.

[3] a) G. Hummer, J. C. Rasaiah, J. P. Noworyta, *Nature* **2001**, *414*, 188; b) A. Kalra, S. Garde, G. Hummer, *Proc. Natl. Acad. Sci. USA* **2003**, *100*, 10175; c) K. Koga, G. T. Gao, H. Tanaka, X. C. Zeng, *Nature* **2001**, *412*, 802; d) D. Takaiwa, I. Hatano, K. Koga, H. Tanaka, *Proc. Natl. Acad. Sci. USA* **2008**, *105*, 39; e) L. Wang, J. J. Zhao, F. Y. Li, H. P. Fang, J. P. Lu, *J. Phys. Chem. C* **2009**, *113*, 5368.

[4] a) J. K. Holt, H. G. Park, Y. M. Wang, M. Stadermann, A. B. Artyukhin, C. P. Grigoropoulos, A. Noy, O. Bakajin, *Science* **2006**, *312*, 1034; b) H. J. Wang, X. K. Xi, A. Kleinhammes, Y. Wu, *Science* **2008**, *322*, 80; c) J. K. Holt, *Adv. Mater.* **2009**, *21*, 3542.

[5] F. Fornasiero, H. G. Park, J. K. Holt, M. Stadermann, C. P. Grigoropoulos, A. Noy, O. Bakajin, *Proc. Natl. Acad. Sci. USA* **2008**, *105*, 17250.

[6] Z. K. Wang, L. J. Ci, L. Chen, S. Nayak, P. M. Ajayan, N. Koratkar, *Nano Lett.* **2007**, *7*, 697; Y. Maniwa, K. Matsuda, H. Kyakuno, S. Ogasawara, T. Hibi, H. Kadowaki, S. Suzuki, Y. Achiba, H. Kataura, *Nat. Mater.* **2007**, *6*, 135; X. S. Li, G. Y. Zhu, J. S. Dordick, P. M. Ajayan, *Small* **2007**, *3*, 595; X. J. Gong, J. Y. Li, H. J. Lu, R. Z. Wan, J. C. Li, J. Hu, H. P. Fang, *Nat. Nanotechnol.* **2007**, *2*, 709.

[7] M. A. Shannon, P. W. Bohn, M. Elimelech, J. G. Georgiadis, B. J. Marinas, A. M. Mayes, *Nature* **2008**, *452*, 301.

[8] M. Mascal, L. Infantes, J. Chisholm, *Angew. Chem.* **2006**, *118*, 36; *Angew. Chem. Int. Ed.* **2006**, *45*, 32.

[9] a) U. S. Raghavender, S. Aravinda, N. Shamala, Kantharaju, R. Rai, P. Balaram, *J. Am. Chem. Soc.* **2009**, *131*, 15130; b) U. S. Raghavender, Kantharaju, S. Aravinda, N. Shamala, P. Balaram, *J. Am. Chem. Soc.* **2010**, *132*, 1075.

[10] A. L. Sisson, V. del Amo Sanchez, G. Magro, A. M. E. Griffin, S. Shah, J. P. H. Charmant, A. P. Davis, *Angew. Chem.* **2005**, *117*, 7038; *Angew. Chem. Int. Ed.* **2005**, *44*, 6878.

[11] The internal diameter of a (6,6) single-walled carbon nanotube, as featured in many simulations,[3] is ca. 5 Å.

[12] For details see the Supporting Information.

[13] Crystal data for **2**: $C_{57}H_{68}N_6O_5$ $2H_2O$, $M = 953.21$; hexagonal, $P6_1$, $a = b = 28.9480(6)$, $c = 11.4319(2)$ Å, $V = 8296.3(3)$ Å^3, $Z = 6$, $\theta_{max} = 27.48°$, Mo$_{K\alpha}$ radiation, $\lambda = 0.71073$ Å, $T = 100$ K, $\mu = 0.076$ mm^{-1}, $\rho_{calc} = 1.142$ Mg m^{-3}. 47396 reflections measured, 12306 unique ($R_{int} = 0.0204$), 658 parameters, and 9 restraints; $R_1 = 0.0485$ $[I > 2\sigma(I)]$, $wR_2 = 0.1478$, GooF = 1.086. CCDC 774502 contains the supplementary crystallographic data for this compound. These data can be obtained free of charge from The Cambridge Crystallographic Data Centre via www.ccdc.cam.ac.uk/data_request/cif.

[14] Materials Studio 4.4, Accelrys Software Inc.

[15] All atoms apart from the water-chain hydrogen atoms were kept stationary during minimization.

[16] Crystal data for **3**: $C_{63}H_{70}N_6O_5{\cdot}2H_2O$, $M = 1027.29$; hexagonal, $P6_1$, $a = b = 29.315(3)$, $c = 11.5430(11)$ Å, $V = 8590.5(14)$ Å^3, $Z = 6$, $\theta_{max} = 65.14°$, Cu$_{K\alpha}$ radiation, $\lambda = 1.54178$ Å, $T = 100$ K, $\mu = 0.620$ mm^{-1}, $\rho_{calc} = 1.189$ Mg m^{-3}. 65842 reflections measured, 8353 unique ($R_{int} = 0.0427$), 713 parameters, and 260 restraints; $R_1 = 0.0639$ $[I > 2\sigma(I)]$, $wR_2 = 0.1801$, GooF = 1.127. CCDC 774503 contains the supplementary crystallographic data for this compound. These data can be obtained free of

charge from The Cambridge Crystallographic Data Centre via www.ccdc.cam.ac.uk/data request/cif.

[17] S. Suzuki, P. G. Green, R. E. Bumgarner, S. Dasgupta, W. A. Goddard, G. A. Blake, *Science* **1992**, *257*, 942; S. Scheiner, T. Kar, J. Pattanayak, *J. Am. Chem. Soc.* **2002**, *124*, 13257; S. Li, V. R. Cooper, T. Thonhauser, A. Puzder, D. C. Langreth, *J. Phys. Chem. A* **2008**, *112*, 9031.

[18] Crystal data for **4**: M: $C_{59}H_{70}N_8O_5 \cdot 2\,H_2O$, $M = 1007.26$; hexagonal, $P6_1$, $a = b = 29.2924(12)$, $c = 11.3062(5)$ Å, $V = 8401.5(6)$ Å^3, $Z = 6$, $\theta_{max} = 27.48°$, $Mo_{K\alpha}$ radiation, $\lambda = 0.71073$ Å, $T = 100$ K, $\mu = 0.079\ mm^{-1}$, $\rho_{calc} = 1.192\ Mg\,m^{-3}$. 47722 reflections measured, 12208 unique ($R_{int} = 0.0369$), 791 parameters, and 9 restraints; $R_1 = 0.0397$ [$I > 2\sigma(I)$], $wR_2 = 0.1115$, GooF = 1.102. CCDC 774504 contains the supplementary crystallographic data for this compound. These data can be obtained free of charge from The Cambridge Crystallographic Data Centre via www.ccdc.cam.ac.uk/data_request/cif.